Journal of Materials Chemistry C

# Poly(ionic liquid)-Based Monodisperse Microgels as a Unique Platform for Producing Functional Nanomaterials



| | |
|---|---|
| Journal: | *Journal of Materials Chemistry C* |
| Manuscript ID: | TC-ART-10-2014-002487 |
| Article Type: | Paper |
| Date Submitted by the Author: | 31-Oct-2014 |




Complete List of Authors:
Cui, Jiecheng; Tsinghua University,
Gao, Ning; Tsinghua University,
Li, Jian; Tsinghua University,
wang, chen; Tsinghua University, chemistry
Wang, Hui; Tsinghua University, chemistry
Zhou, Meimei; Tsinghua University, chemistry
Zhang, Meng; Tsinghua University, chemistry
Li, Guangtao; Tsinghua University, Chemistry


SCHOLARONE™
Manuscripts

Journal Name

RSCPublishing

ARTICLE

# Poly(ionic liquid)-Based Monodisperse Microgels as a Unique Platform for Producing Functional Materials†

Cite this: DOI: 10.1039/x0xx00000x

Jiecheng Cui,[#] Ning Gao,[#] Jian Li, Chen Wang, Hui Wang, Meimei Zhou, Meng Zhang and Guangtao Li*

Received 00th January 2012,
Accepted 00th January 2012

DOI: 10.1039/x0xx00000x

www.rsc.org/

In this work, we report the microfluidic preparation of monodisperse imidazolium-based poly(ionic liquid) (PIL) microgels with controlled size and morphology, and show that the imidazolium units in microgel network can be exploited as reactive sites to efficiently access desired functional materials by simple counteranion-exchange or conversion reaction. Moreover, based on the counteranion-exchange reaction, spatio-temporal engineering of the surface of the PIL microgels could also be realized, and a new and simple strategy for the fabrication of diverse anisotropic microgels (patchy particles) with great flexibility was developed. Additionally, by exploiting the convenient generation of carbene units from imidazolium moieties as well as the carbonizable feature of PIL, the prepared PIL microgels could be further converted into stable carbene spheres and monodisperse carbon particles. All results show that these monodisperse PIL-based microgels can serve as a very useful platform for facilely accessing various functional materials.

## Introduction

Polymer microgels are micrometer-sized particles, which have a three-dimensional network structure and are inflated with a solvent.[1] Due to their unique structural features, microgels have gained increasing attentions over the past years and have been exploited for various applications in drug delivery, chemical sensing, separation and purification techniques, fabrication of photonic crystals, and catalysis for organic and inorganic synthesis.[2] Recently, due to promising applications as smart nanoreactors, the introduction of metal nanoparticles into polymer microgels to produce hybrid microgels have attracted considerably attentions.[3] However, to achieve microgels with desired function as well as sufficient mechanical strength, traditionally each fabrication is strongly dependent on the screening and arduous synthesis of functional monomer as well as the optimization of polymerization conditions. Especially in the case of sensitive functional moieties (e.g. bioactive units) incompatible with the conventional thermal- or photo-induced polymerization process, the traditional polymerization methods are inappropriate or difficult for fabricating the corresponding microgels. Thereby, developing a new strategy to efficiently access monodisperse functional microgels with controlled sizes and morphologies is highly desirable.

Ionic liquids (ILs), a class of salts composed of discrete organic cations and anions, exhibit a series of unique properties including negligible vapor pressure, non-flammability, high ionic conductivity, a wide electrochemical window, and good chemical and thermal stability.[4] Importantly, such favorable properties can be individually manipulated through modulating the combination of cations and anions, providing unprecedented tunability.[5] Thereby, these distinct physiochemical properties and features make ILs ideal candidates for the design and development of functional materials and chemical systems. Some studies have demonstrated the applications of ionic liquids or their polymers (PILs) in fabrication of functional materials through the counteranion-exchange reaction.[6,7] However, few work has been reported on multifunctional microgels as well as patchy microparticles, which present an exciting new research area and have attracted a large amount of attention due to their strongly anisotropic and directional interactions.[8] In this respect, there are still some challenges need to face. More importantly, the properties of ionic liquids are actually much more than the counteranion exchange feature. Especially, in the case of the imidazoulium-based PILs, the imidazoulium moiety is not only "reactive site" for counteranion exchange, but also can serve as carbene and carbon precursors.[4,9] It can be conceivable that the exploitation of these unique properties of imidazoulium moiety should open up an efficient avenue to access various functional microgels and materials from one PIL-based microgels.

Inspired by the unique properties of ILs, herein we report on

Journal Name RSCPublishing

ARTICLE

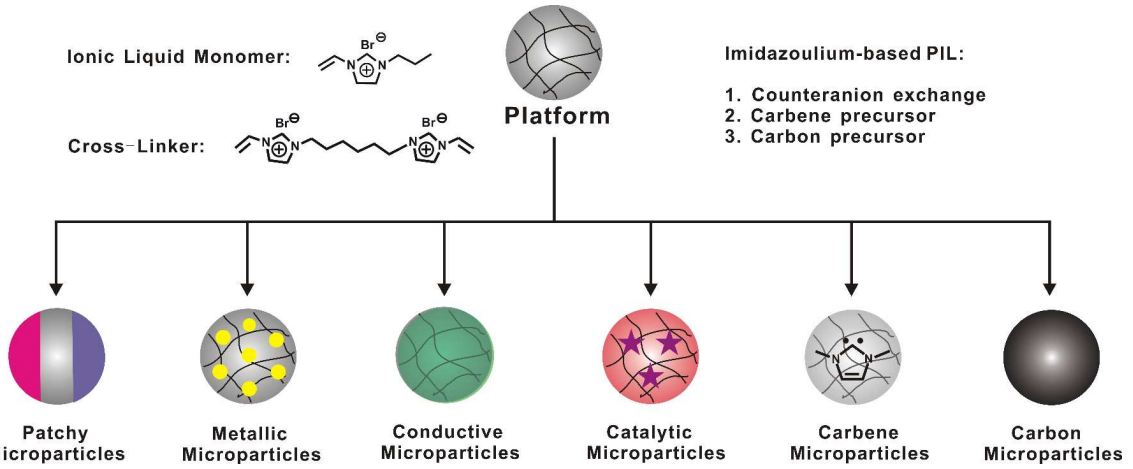


**Scheme 1.** Poly(ionic liquid)-based monodisperse microparticles as a unique platform for producing functional materials including patchy particles, metal-containing microgels, conductive composite particles, catalytic particles, carbene particles, and carbon particles.

the microfluidic synthesis of monodisperse imidazolium-based PIL microgels, and show that the imidazolium units in the resultant polymer network indeed can be exploited as functional sites to efficiently access desired functional materials by not only the simple counteranion-exchange, but also conversion reaction. As demonstration, three types of isotropic functional particles, including metal-polymer hybrid particles, conductive composite particles and catalytic particles, were first evolved from the prepared PIL microgels. More importantly, based on the "task-specific" concept of ILs,[7] the surface of the PIL microgels could be spatio-temporally engineered to afford multifunctional as well as patchy microparticles. Thus, a new and efficient strategy was developed to realize the fabrication of multifunctional patchy microparticles with great flexibility. Additionally, due to the convenient generation of carbene units from imidazolium moieties as well as the carbonizable feature of PIL, the prepared PIL microgels could be further converted into stable carbene spheres and monodisperse carbon particles. Actually, these monodisperse PIL-based microgels can serve as a useful platform for facilely accessing various functional materials (Scheme 1).

## Results and discussion

### Synthesis of the monodisperse PIL-based microgels

Microfluidic synthesis of microgel particles begins with the emulsification of a precursor solution in an immiscible liquid. The resulting particle dimensions and their uniformity are pre-determined in the stage of microfluidic emulsification. In the previous works,[10] it is verified that the diameter of the formed precursor droplets ($D_d$) (and hence, the corresponding solid particles) is sensitive to a number of preparation parameters, including the caliber of the glass capillary microchannel ($D_g$), the viscosity of the continuous phase ($u_c$) and dispersed phase ($u_d$), the flow velocity of the continuous phase ($v_c$) and dispersed phase ($v_d$), and the interfacial tensions between the continuous and dispersed phases. Recently, C. Serra and his coworkers established that the diameter of the resulting droplets in microfluidic emulsions is a function of the channel dimensions, the flow rates, viscosities, and interfacial tensions of the continuous and dispersed phases, as follows:[11]

$$D_d / D_g = K(Ca_c / Ca_d)^M$$

where K and M are constant, $Ca_c$ and $Ca_d$ are the capillary number for the continuous phase and the dispersed phase, and $Ca_c = u_c v_c/\gamma$, $Ca_d = u_d v_d/\gamma$, $\gamma$ is the interfacial tension. Obviously, for a given emulsion system in a microfluidic device, the dimensions of the formed particles can be controlled by tuning the flow rates of the continuous and dispersed phases.

In the present work, a co-flowing microfluidic device was employed to produce droplets with narrow size distribution, as shown in Scheme S1. Poly(dimethylsiloxane) with surfactants was used as the continuous oil phase, and the dispersed phase was aqueous solution of 1-butyl-3-vinylimidazolium as monomer and 1,6-di(3-vinylimidazolium) hexane as cross-linker (Scheme 1). As previously reported work,[11] the diameter of the droplets increases when the flow rate of the dispersed phase increases or when the flow rate of the continuous phase decreases. Actually, since the velocity ($v_d$) of the dispersed phase is much lower than that of the continuous phase, control of the continuous phase velocity is found to be more practically useful means for generating droplets with good controlled

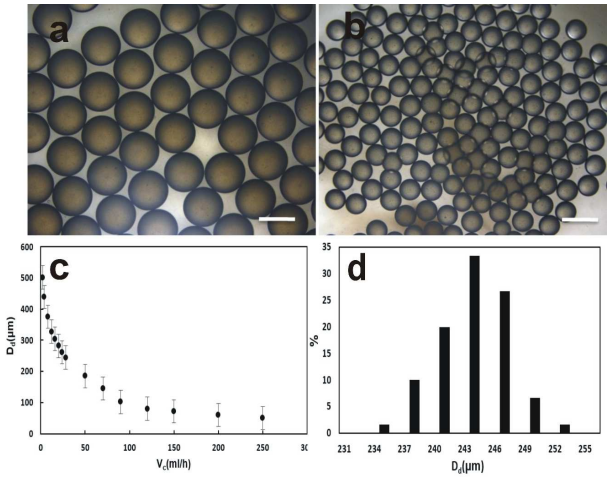


**Figure 1.** Optical images of the fabricated PIL microgels with a diameter of 467μm (a) and 233 μm (b). The scale bar is 450μm; c) Relationship between the diameter of the droplets $D_d$ and the flow velocity of the continuous phase($v_c$) under conditions: vd=0.5 mL/h, $D_g$=120 μm and 50cSt silicon oil as continuous phase; d) Size distribution of microgels, the mean diameter and coefficient of variation of the formed microgels (244 μm).

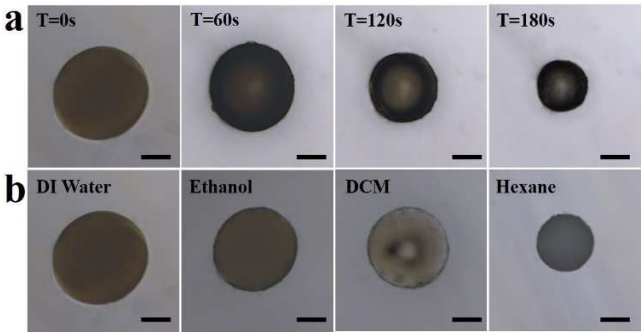


**Figure 2.** a) Size evolution of the swollen PIL microgels exposed to the air; b). Swelling of the prepared PIL particless exposed to different organic solvents. Scale bar is 100 μm.

bead size and high repeatability. Thus, in this work, the control of the flow rates of the continuous and dispersed phases was employed to realize the creation of microgel particles with different sizes. The microgels of 467μm were obtained when the $v_d$=0.5 mL/h and $v_c$=25mL/h were used (Figure 1a). As mentioned above, regulation of the flow rate of the continuous phase provides more effective control over the size of the resulting microgel particles. When the flow rate of the continuous phase was increased from 25 mL/h to 100mL/h, the microgels with an obvious smaller diameter (233μm) was obtained (Figure 1b). Figure 1c shows the correlation between the flow velocity of the continuous phase ($v_c$) and the sizes of the formed droplets ($D_d$) under conditions: vd=0.5 mL/h, $D_g$=120 μm and 50cSt silicon oil as continuous phase. Clearly, it can be seen that with increased flow velocity of the continuous phase, the diameter of the formed droplets gradually decreases. Certainly, the viscosity of the continuous phase has also an obvious effect on the droplet size. Generally, a high viscosity of the continuous phase leads to a smaller particle diameter, due to the relative increase of the shear force exerted on the dispersed phase by the continuous phase over the interfacial force. In our case, the dispersion of particle sizes is quite

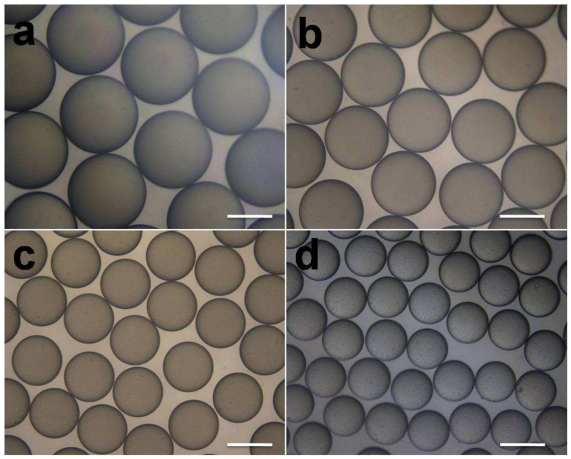


**Figure 3.** Optical images of the PIL microgels with different counteranions: a) microgels with Br- as counteranions (diameter: 370 μm); b) microgels with $BF_4^-$ as counteranions (diameter: 305 μm); c) microgels with $PF_6^-$ as counteranions (diameter: 236 μm); d) microgels with $Tf_2N^-$ as counteranions (diameter: 189 μm). The scale bar is 200 μm.

low (Figure 1d). Under optimized conditions the microfluidic generation of polymer particles with polydispersity below 1-2% is possible. These results indicate that by using a simple microfluidic system monodisperse PIL microgels with controlled sizes could be facilely fabricated. In our case, the value of M in the above mentioned equation was determined to be -0.27 by analyzing the parameter $D_d$, $D_g$, $v_c$, $v_d$, $u_c$, and $u_d$ in the size control experiments of microgels.

As expected, the prepared PIL particles exhibit characteristic feature of microgels. The original PIL particles (with $Br^-$ as counteranions exhibited considerable swelling in water or water solution. Upon exposure to air atmosphere, the swollen PIL particles gradually became smaller with the loss of water molecules (Figure 2a) and their size dramatically changes from swollen to dried state, for example from 850 μm to 230 μm. The swelling and deswelling process is completely reversible. Additionally, it is found that upon exposure to different organic solvents, the prepared PIL particles exhibit different swelling (Figure 2b).

### Counteranion-exchange behavior of the PIL microgels

As mentioned in Introduction, one of the most attractive feature of ILs is that their physicochemical properties and functionality can be easily tailored by simply counteranion exchange. Thus, the counteranion-exchange behavior of the prepared PIL microgels (with Br- as counteranion) was first examined by using three salts, including sodium tetrafluoroborate ($NaBF_4$), lithium bis(trifluoromethane sulfonimide) ($LiTf_2N$) and sodium hexafluorophosphate ($NaPF_6$)(Scheme S2). As expected, upon exposure of the fabricated microgels to an aqueous solution of the chosen salts, gradual shrinkage of their sizes was observed, indicative of the occurrence of the counteranion-exchange reaction. With the displacement of Br- by hydrophobic anions, the prepared PIL microgels become smaller. The more hydrophobic the used counteranion is, the smaller the microgels became (Figure 3). The counteranion-exchange reaction seems

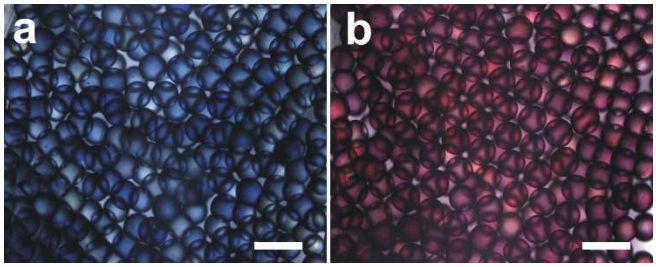


**Figure 4.** Optical images of the fabricated PIL microgels after the exposure to indigo carmine (a), and spadns (b) aqueous solution, respectively. The scale bar is 500μm.

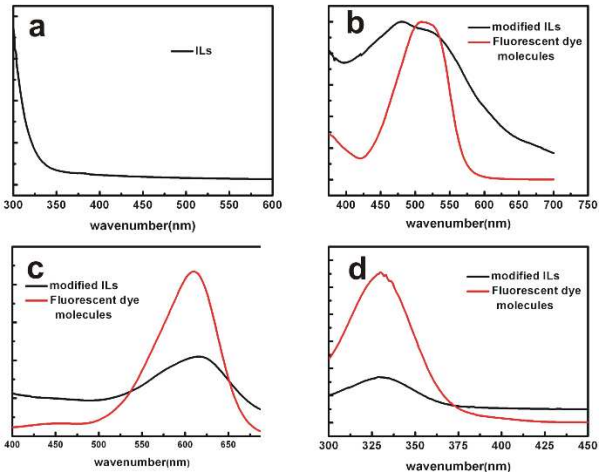


**Figure 5.** UV/vis spectra of the fabricated PIL microgels before and after the treatment with aqueous solution of different dye molecules: a) original PIL microgel; b) treated with spadns; c) treated with indigo carmine; d) treated with 9,10-anthraquinone-2-sulfonic acid sodium salt. For comparison the UV/vis spectra of the used dye molecules were also include, respectively

relatively fast and took about two hours for the used microgels. Indeed, the FT-IR analysis confirmed the occurrence of the anion exchange and the existence of the chosen anions. Figure S1 in Supporting Information shows the comparison of the FT-IR spectra of the PIL microgel particles before and after the exposure to different anion aqueous solutions. It is clearly seen that the characteristic absorption bands of the used anions were detected at 1083cm$^{-1}$ ($BF_4^-$), 838cm$^{-1}$ ($PF_6^-$), 1356 cm$^{-1}$ ($Tf_2N^-$), respectively.[12]

To visualize the anion-exchange process, in this work, three typical dye molecules (Spadns, 9,10-Anthraquinone-2-sulfonic acid sodium and Indigo carmine in Scheme S2) were employed to further confirm the feasibility of the introduction of specific function in the PIL microgels by anion-exchange reaction. Similarly, the prepared PIL microgels ($Br^-$ as counteranion) were soaked in aqueous solution of the corresponding dye molecule at room temperature for 12 h. After filtered off, the treated PIL microgels were washed thoroughly to remove the physically trapped dye molecules until no coloration was observed in washing solution. As shown in Figure 4, the treated PIL microgels, exhibiting a clear color throughout the microgels, display different appearance from the original PIL microgels which don't exhibit optical property (Figure 1). Figure 5 shows

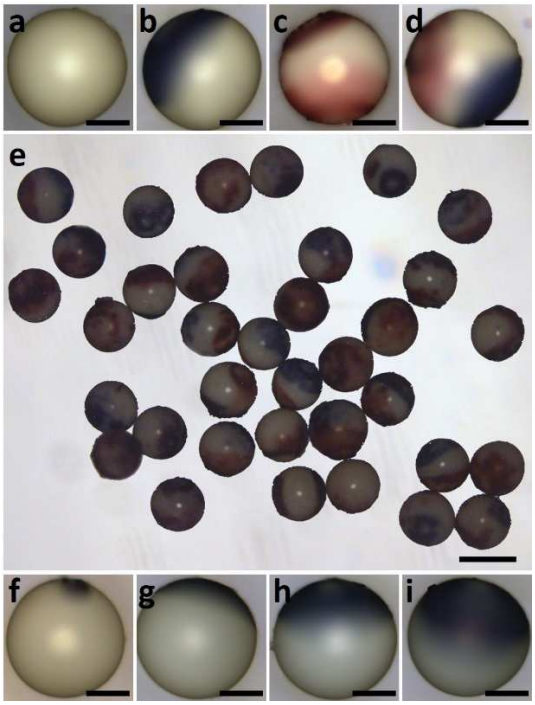


**Figure 6.** Optical images of the original PIL microgel (a) and the derivated patchy particles with A-B structure (b), with A-B-A structure (c) with A-B-C structure (d,e); the microgels with tunable patchy size(f-i).The scale bar is 100μm(a-d,f-i), 300μm(e), respectively.

the UV-vis spectra of the used dye molecules and the PIL microgels before and after the counteranion-exchange treatment. Obviously, by simple anion-exchange the optical properties of functional anions were correctly introduced into the PIL microgels. These results clearly indicate that the counteranion-exchange property of the ionic-liquid units inside PIL microgels is still retained, and the functional groups could be facilely introduced into the prepared microgels via anion-exchange reaction.

### Preparation of patchy microgels or particles through spatio-temporal engineering of the surface of the PIL microgels

Compared to monofunctional microgel particles described above, the multifunctional microgels as well as anisotropic patchy particles are another more interesting class of particles that exhibit completely different properties and hold numerous promising applications.[13] In this respect, the surface of PIL microgels were designed by spatio-temporal engineering to achieve the multifunctional microparticles as well as patchy particles. Due to the counteranion-exchange capability of ionic liquids, the PIL also show great flexibility in surface chemistry engineering, and allow for producing various multifunctional anisotropic structures. By using a "sandwich" microcontact printing (μCP) (Scheme S3) method,[14] the PIL microgels with A-B, A-B-A, or A-B-C patchy structure were easily accessible (Figure 6). In this work, for visual inspection two fluorescent counteranions (Indigo carmine and Spadns) were used as chemical "ink" and the PDMS elastomer was utilized as a stamp. It is found that the printing process in our case


This journal is © The Royal Society of Chemistry 2012

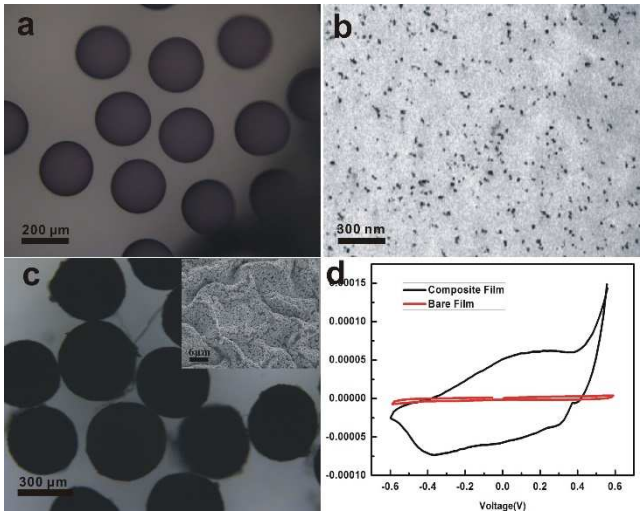


**Figure 7.** a) Optical image of the microgels containing Au nanoparticles; b) TEM image of the microgels containing Au nanoparticles; c) Optical image of the conductive microgels; Inset is the SEM image of the prepared conductive particles, d) Cyclic voltammograms of the original PIL microgel and the resulting composite conductive particles.

proceeded very fast at room temperature. It took only several minutes to transfer the "ink" to PIL microgels via counteranion-exchange exclusively in the area of contact. The contact time and pressure could be used to turn the size of the formed patchy (Figure 6f-i). Due to the unlimited combination of cation and anion,[5] although only fluorescent anisotropic PIL microgels were fabricated, principally unlimited PIL patchy particles can be easily accessible through simple counteranion-exchange reaction, including biomolecule-binding patchy particles and magnetic patchy particles. Compared to numerous developed approaches,[13] the spatio-temporally engineered surface strategy described here is simple and versatile, offering a broad design space for fabricating desired multifunctional materials (patchy microparticles) under mild conditions.

**Fabrication of various functional microgels using PIL microgels.**

Based on the concept of "task-specific" ionic liquids,[7] a variety of functional groups as anions can be readily introduced into the PIL-IOMS by simply anion-exchange reaction, leading to new microgels or spheres with desired functions. Thus, the immobilization of metal nanoparticles in microgels through the counteranion exchange reaction followed by reduction of the incorporated metallic complex is possible. The uniform and homogenous metal-polymer hybrid microgels has fascinated recently scientists, due to their potential applications in chemical sensing or as nanoreactors. Under this consideration, in our work, the Au-PIL hybrid microgels were synthetized by introducing precursor $AuCl_4^-$ anion into PIL microgels via counteranion exchange and subsequent reduction using $NaBH_4$ as reducing agent (Scheme S4). Figure 7a-b shows the optical and TEM images of the prepared Au-PIL hybrid microgels. Compared to the original PIL microgels (with $Br^-$ as anion), the resultant microgels show considerable shrinking of particle size and exhibit purple color in appearance, indicative of the

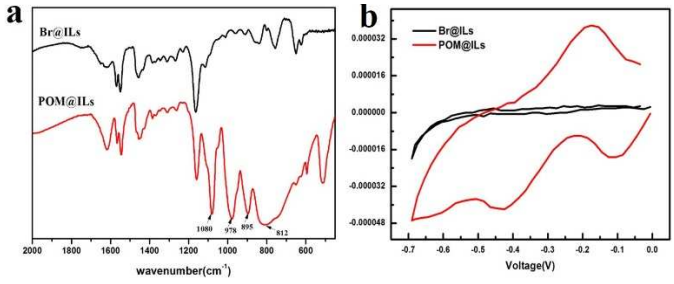


**Figure 8.** a) FT-IR spectra of the fabricated PIL microgels before and after the treatment with aqueous solution of peroxotungstate; b)Cyclic voltammograms of the original PIL microgels before and after the counteranion exchange with POM.

formation of gold nanoparticles (Figure 7a). Under TEM observation, a large number of gold dark dots with a diameter of about 20 nm were detected to be homogeneously distributed inside of the PIL microgels (Figure 2b). Figures S2 and S3 show TGA and EDX spectrum of the prepared Au-PIL hybrid microgels. TGA measurement demonstrates that 2 wt% Au nanoparticles have been immobilized into PIL microgels. Meanwhile, the content of the Au nanoparticles can be up to 6 wt% through adjusting the amount of $AuCl_4^-$ introduced during the counteranion exchange reaction. Interestingly, it is found that the trapped Au nanoparticles in PIL gels display remarkable stability and no leakage and aggregation of the Au nanoparticles were detected with the prolonged storage of the hybrid microgels in water. Recently, numerous works reported the similar phenomenon that some ionic liquids, especial the imidazolium-based ionic liquids, can hold stable suspensions of metallic nanoparticles without additional surface-active agents.[15] By means of XPS and Raman analysis, several studies suggest that in the case of imidazolium-based ionic liquids, strong interaction between metal particles with positively charged imidazulium rings is present, which is responsible for the solvation and stability of nanoparticles in ionic liquids. Based on these results, we believe that the same stabilization mechanism could be used to explain the observed phenomenon in our case. Additionally, after the displacement of Br- by $AuCl_4^-$ anions followed by the reduction by using $NaBH_4$, (Scheme 4), it was found that the resulting Au-containing microparticles have smaller size compared to the original microgels (with Br- as anion). The exact reason for this phenomenon is still not clear. Probably, the strong interaction between gold particles with IL moieties makes the size of the resulting composite particles reduced.

Interestingly, we found that the $AuCl_4^-$ anions incorporated into PIL microgels could also serve as reduction agents to produce uniform conducting polymer spheres, when the PIL microgels were exposed to the solution of pyrrole. Figure 7c displays the optical image of the resulting conductive hybrid particles, which shows quit different morphology from the original microgels. In particular, under SEM observation the obtained conducting polymer (polypyrrole) microparticles shows typical granular morphology (Inset in Figure 7c), and polypyrrole coating on the surface is very evident. Importantly, electrochemical analysis of the formed particles provide a direct

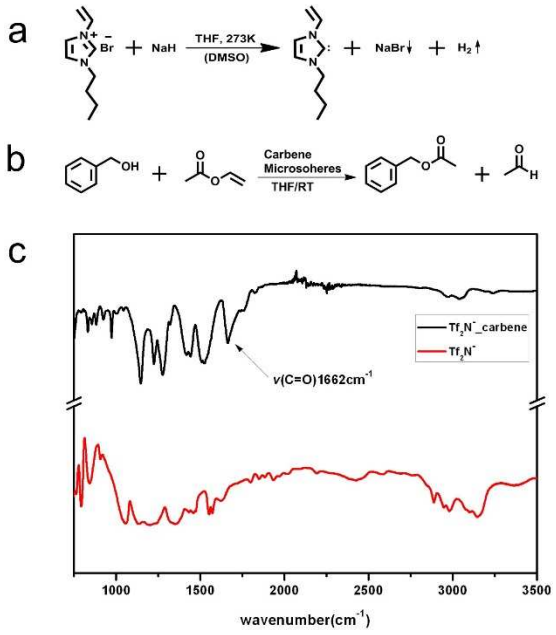


**Figure 9.** Model reaction for synthesis of Crabene(a) and the evaluation of the catalytic capability of the carbene microspheres(b); (c) FT-IR spectra of the prepared carbene microspheres before and after the reaction with $CO_2$.

evidence for the formation of conductive polypyrrole inside particles. As shown in Figure 7d, the redox behaviour of polypyrrole composite spheres was investigated by cyclic voltammetry. Compared to the original microgels, which don't exhibit any electrochemical activity in the range from -0.6V to 0.6V, the resulting composite spheres show characteristic redox feature of polypyrrole.

As a further demonstration, polyoxometalates (POMs) were chosen as task-specific building blocks and introduced into the PIL microgels. POMs are a family of anionic, inorganic metal oxide, and exhibit a wide range of topologies and very rich redox chemistry that provides the basis for their high catalytic activity in oxidation reactions.[16] The combination of organic cations of the PIL microgels with POM anions could not only lead to the formation of recoverable catalysts, but also the microgels with electrochemical activity (Figure 8). In our case, the dinuclear peroxotungstate $[\{W(=O)(O_2)_2(H_2O)\}_2(\mu\text{-}O)]^{2-}$ [17] was used as catalytic anion, due to its high efficiency of $H_2O_2$ utilization and high selectivity to the epoxides.[16] The incorporation of the PIL microgels with peroxotungstate was simply achieved through the exposure of the PIL microgels into an aqueous solution of potassium salt of peroxotungstate at RT for 12 h. FT-IR measurements confirmed the correct loading of peroxotungstate active species into the interior of the PIL microgels. Compared to the FT-IR spectrum of the original PIL microgels, the characteristic bands[18] of peroxotungstate at 1080 cm$^{-1}$, 978 cm$^{-1}$, 895 cm$^{-1}$, and 812 cm$^{-1}$ were detected in the treated samples (POM@PIL) (Figure 8a). The catalytic performance of POM@PIL microgels was evaluated by using the oxidation reaction of olefins. Concretely, POM@PIL microgels were dispersed in acetonitrile solution of cyclooctene with hydrogen peroxide as an eco-friendly oxidant. The

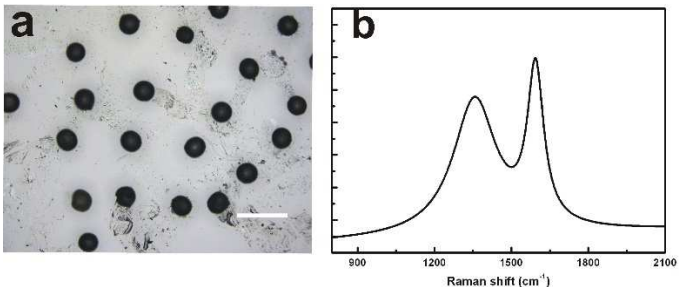


**Figure 10.** a) Optical image of the resulting carbon spheres; b) Raman spectrum of the resulting carbon spheres. The scale is 200μm.

oxidation reaction was carried out at 333K under stirring. At given time intervals of reaction, the product and yield were determined by GC/MS analysis. It is found that POM@PIL microgels exhibited excellent catalytic activity. After 5 hours 93% of cyclooctene were converted into the corresponding epoxides. The above results indicate that the observed catalysis indeed originates from the ionic bonded peroxotungstate species and the catalysis of the POM@PIL microgels is truly heterogeneous in nature. As a control experiment, the same reaction mixture only without POM@PIL microgels was stirred at 333 K for 5h. As expected, the conversion was as low as 1.77%. Additionally, the catalytic property of the POMs incorporated microgels was compared with that of pure POMs under the same conditions. It was found that 98% of cyclooctene were converted into the corresponding epoxides by using pure POMs. This result indicates that the catalytic performance of the POMs remain nearly unchanged after their incorporation into microgels.

**Fabrication of uniform carbene spheres from PIL microgels**

Since the first isolation and characterization of stable N-heterocyclic carbenes (NHCs) by Arduengo in 1991, these compounds have attracted great interest in various fields of chemistry.[19] As molecules with divalent carbon atoms, NHCs are not only of theoretical interest but also of practical relevance as versatile ligands and effective organocatalysts. In our work, we found that the PIL microgels produced from the imidazolium-based IL mononer can be readily transformed to stable N-heterocyclic carbine microspheres by deprotonation of imidazolium moieties with sodium hydride in tetrahydrofuran in the presence of a catalytic amount of dimethyl sulfoxide (Figure 9a).[19] Because of their high basicity, N-heterocyclic carbenes can react rapidly with $CO_2$ to afford zwitterionic adducts (designated as NHC-$CO_2$), even at very low $CO_2$ concentrations. Indeed, it is found that the resultant carbene spheres can be used as a highly efficient adsorbent for reversible fixation-release of $CO_2$. Figure 9c shows the FTIR spectra of the microspheres before and after the reaction with $CO_2$. The appearance of the asymmetric ν($CO_2$) vibrations of NHC-$CO_2$ adduct at 1649 cm$^{-1}$ confirmed the presence of NHC moieties in microspheres.[20] As expected, the produced carbene microspheres show excellent catalytic effect for transesterification and acylation reactions. In our case, a simple

 This journal is © The Royal Society of Chemistry 2012

transesterification of benzyl alcohol and vinyl acetate in tetrahydrofuran was performed in the presence of the carbene spheres and under nitrogen atmosphere (Figure 9b). Concretely, Monodisperse carbene spheres were dispersed in tetrahydrofuran solution of benzyl alcohol and vinyl acetate. The reaction was carried out at 298 K under stirring. At given time intervals of reaction, the product and yield were determined by GC/MS analysis. After 10mins, the reactants were quantitatively converted into product. It indicated that the carbene spheres exhibited excellent catalytic activity. In contrast, the same reaction didn't occur without the assistance of the carbene spheres. Probably due to the steric hindrance offered by the polymeric network, the obtained carbene microspheres show remarkable stability and could serve as recoverable catalysts. As a control experiment, the catalytic property of pure NHCs was also studied under the same conditions. It was found that the catalytic performance of the NHCs remain nearly unchanged after their incorporation into microgels.

**Fabrication of uniform carbon spheres using PIL microgels**

The unique features of ionic liquids mentioned in introduction section have rendered the wide use of ILs in many areas, for instance, as materials for fabricating different kind of functional materials through the counteranion-exchange, as solvents for organic and inorganic synthesis, as electrolytes for energy applications. In an effort to expend new applications, ionic liquids and their polymers have been found to be excellent precursors for producing functional carbon materials.[4b] Figure 10 shows the optical image of the carbon microspheres produced from carbonizing the PIL microgels at 1073K under $N_2$ atmosphere. Obviously, all the carbon spheres preserve a spherical morphology and have a narrow size distribution. However, considerable shrinkage of particle size occurred during the carbonization process and the diameter of the resultant carbon particles is much smaller than that of the parent particles. For example, the carbonization of the PIL microgels with a diameter of 420μm afforded 80μm carbon spheres. Nevertheless, this result indicates that different monodisperse carbon particles can be readily fabricated by choosing PIL microgels with different particle size. The cross-linked polymer structures and surface tension of the microgels, are the principal reason for the retention of spherical morphology under the high-temperature annealing.

Raman spectrum of the obtained carbon spheres reveals two distinct peaks at 1350cm$^{-1}$ and 1580cm$^{-1}$ (Figure 10b), confirming the presence of amorphous and graphitic carbon domains.[21] The 1580cm$^{-1}$ band is associated with a graphitic carbon with $sp^2$ electronic configuration. The band at 1350 cm$^{-1}$ arises from polycrystalline graphite, and can be attributed to diamond like carbon atoms with $sp^3$ configuration. Earlier work in our laboratory suggested that the area ratio of $Asp^3$ to $Asp^2$ decreased with increasing carbonization temperature.[22] Thus, the carbonization of the PIL microgels at higher temperature can lead to further graphitized structures.

## Conclusions

In summary, by using microfluidic approach, we successfully produced monodisperse poly(ionic liquid) microgels with controlled size and morphology. Based on the utilization of the unique properties of poly(ionic liquid), such as spatio-temporal engineering of microgels' surface through counteranion exchange reaction, imidazolium-based conversion reaction as well as carbonizable feature, it is found that the poly(ionic liquid) microgels could be easily evolved for conveniently fabricating functional materials with a variety of potential applications. Due to the unlimited combination of cation and anion, principally unlimited PIL multifunctional materials as well as anisotropic patchy particles can be easily accessible. The imidazolium-based conversion reaction of poly(ionic liquid) provides another opportunity to construct unique carbene microspheres with remarkable stability, showing promising catalytic applications as heterogeneous catalyst. Additionally, the carbonizable feature of poly(ionic liquid) allows for efficiently producing monodisperse carbon particles. All obtained results clearly indicate that as a unique platform these poly (ionic liquid) microgels could provide tremendous opportunities, principally unlimited possibilities, for facilely accessing various functional materials.

## Experiment Section

**Chemicals:**

All solvents and chemicals are of reagent quality and were used without further purification unless special explanation. 1-vinylimidazole, 1-bromobutane 1,6-dibromohexane, were purchased from Alfa and used as received. Silicon oil (20cSt, 50cSt), 2,2-Azobis(2-methylpropion-amidine) dihydrochloride (AIBA) as photoinitiator were purchased from Aldrich. Polydimethylsiloxane (KF-96 10cSt) was gained from Shin-Etsu Chemical, Japan. Silicon oil and span80 were brought from Yunuo Chemicals Ltd, China.

**Instrumentation:**

1H NMR spectra were obtained by a JEOLJNMECS 300NMR spectrometer. UV-vis spectra were carried out by a PerkinElmer Lambda35 spectrometer. The photopolymerization was carried out under UV light. The microstructures of the beads were characterized by a scanning electron microscopy (SEM, HITACHI, S-300N). Photographs of the beads were taken with an optical microscope (OLYMPUS BXFM) equipped with a CCD camera. The microfluidic devices were homemade by glass capillary tubes with inner diameter of 75 μm and outer diameter of 200 μm and a T-junction. The monomer dispersed phase and oil continuous phase are delivered by syringe pumps. The dispersed phase was injected via a glass capillary tube positioned along the main axis of the T-junction. The continuous phase is injected perpendicular to the main axis of the T-junction.

**Synthesis of Ionic Liquid Monomers:**

The ionic liquid monomer, 1-Butyl-3-vinylimidazolium bromide, was synthesized according to literature,[23] 1-Vinylimidazole (6.00 g, 64 mmol) was mixed with 1-bromobutane (10.5 g, 76.8 mmol), and the mixture was stirred vigorously at 343K. After 3 h reaction, the residual 1-bromobutane was removed under vacuum at 333K to afford a yellow solid. The dicationic 1,6-di(3-vinylimidazolium)hexane bromide as crosslinker was synthesized as follows. A mixture of 2 molar equivalents of 1-vinylimidazole and 1 molar equivalent of 1,6-dibromohexane was stirred at room temperature until the IL solidified. Then the bromide salt was dissolved in water, the mixture was washed with ethyl acetate three times to remove impurities. The last residue was evaporated in vacuum to ensure complete dryness. 1H NMR (300 MHz, DMSO-d6, δ): 9.56 (s, 2H, -NCHN-), 8.22(s, 2H, -NCHC-), 7.95(s, 2H, -CCHN-), 7.31 (m, 2H, -CH=$CH_2$), 5.97(dd, J = 2.4Hz, J = 15.8Hz, 2H, -HCH=CHN-), 5.44(dd, J = 2.07Hz, J = 6.54Hz, 2H, -HCH=CHN-), 4.21(t, J = 7.2Hz, 4H, -$NCH_2CH_2$), 1.84(t, J = 6.87Hz, 4H, $NCH_2CH_2CH_2$), 1.31(m, 4H, -$CH_2CH_2CH_2$-).

**Preparation of monodisperse PIL microgels:**

1.2 g IL monomer and 0.4g crosslinker were dissolved in 400ul water containing 2, 2-Azobis(2-methylpropion-amidine) dihydrochloride (AIBA) as photoinitiator. To produce monodisperse PIL microgels, the homemade microcapillary devices were used as shown in Scheme 1. The oil phases was poly(polydimethylsiloxane) with span80 as Stabilizer. We pumped the aqueous solution of ILs and oil phases into the inner and outer capillaries at volumetric flow rates of about 0.5mL/h and 50mL/h, respectively. Then the aqueous flow was broken into droplets by the oil flow at the needle tip. The generated droplets were solidified by photopolymerization under UV exposure less than 1 min and the resulting PIL microgels were taken into the collection container filled with the oil by the oil flow. The generated PIL microgels were rinsed with hexane, deionized water several times, to remove the silicon oil and the residual surfactant.

**Monodisperse PIL microgels as platform to produce functional materials:**

**A) Patchy microgels:** The Patchy PIL microgels were fabricated with a versatile strategy by using a "sandwich" contact printing (μCP) method. The PDMS stamps were loaded with a few drops of the respective chemical ink solution ($10^{-8}$ mM, aqueous solution of fluorescent dye molecules) and the excess ink solution was removed under a stream of argon. Then the PIL microgels were loaded onto the stamp and a second stamp, loaded with the second ink (like the first one) was put on top using a press. The samples were left to react at the room temperature. It took several minutes to transfer the "ink" to PIL microgels via counteranion-exchange only in the area of contact.

**B) Au-polymer hybrid microgels:** The Au-polymer hybrid microgels was also conveniently completed through an anion-exchange reaction and redox reaction. The ILs microgels were added to an aqueous solution of Chloroauric acid at room temperature for 12 h. Then the microgels were immersed into the aqueous solution of sodium borohydride to reduce Chloroauric acid. Then the Au-polymer hybrid microgels were the filtered off, purified by extensive deionized water several times.

**C) Conductive hybrid microgels:** The conductive hybrid microgels was also conveniently completed through an anion-exchange reaction and redox reaction. The ILs microgels were added to an aqueous solution of Chloroauric acid at room temperature for 12 h. Then the microgels were immersed into the solution of pyrrole to obtain a polypyrrole film coating on the surface of the microgels. Then the conducting polymer hybrid microgels were the filtered off, purified by extensive deionized water several times.

**D) Catalytic microgels:** The prepared PIL microgels were added to an aqueous solution of peroxotungstate (POM) at room temperature for 12 h. Then the microgels were filtered off, washed with deionized water several times, and dried in vacuo to afford PIL microgels loaded with peroxotungstate. The potential of the POM-loaded microgels for catalytic applications was ckecked as follows. The PIL microgels loaded with POM were dispersed in acetonitrile solution (1 ml) containing cyclooctene (0.2307 g, 2.1 mmol), hydrogen peroxide (30% aq. solution, 0.0647 g). Then the reaction mixture was stirred at 333 K for 5h. After the reaction was finished, the ILs microgels were separated by the filtration, washed with the solvent, and dried in vacuo prior to being recycled.

**E) Carbene microspheres:** The Carbene microspheres were obtained by the treatment of the imidazolium-based PIL microgels with NaH in THF at 273K (Catalytic amount of DMSO) under $N_2$ atmosphere.

**F) Carbon Particles:** The PIL microgels were first immersed in aqueous solution of the $FeCl_3$ for 3h, and then after washing and dired in air the treated microgels were heated under $N_2$ atmosphere to 623K with a heating rate of 1K $min^{-1}$, then maintained at 623K for 2 h, and subsequently heated to 1073K with a heating rate of 1K $min^{-1}$ and kept at 1073K for 5 h. Then the resulting carbon particles were taken out and cooled to room temperature.

## Acknowledgements

We gratefully acknowledge the financial support from the NSFC (21025311, 21121004, 21261130581, 91027016), Ministry of Education (2011Z01014), MOST (2011CB808403, 2013CB834502) and the transregional project (TRR61).

## Notes and references

Department of Chemistry, Key Lab of Organic Optoelectronics & Molecular Engineering, Tsinghua University, Beijing 100084, P. R. China. E-mail: LGT@mail.tsinghua.edu.cn Fax: (+86) 10-6279-2905.

# These authors contribute equally to this paper

 This journal is © The Royal Society of Chemistry 2012

† Electronic Supplementary Information (ESI) available: details of any supplementary information available should be included here]. See DOI: 10.1039/b000000x/

1 B. R. Saunders, B. Vincent, *Adv. Colloid Interface Sci.* **1999**, 80,1.

2 a) Y. Lu, N. Welsch, M. Ballauff, *Chemical Design of Responsive Microgels*, *234*, Springer, Berlin **2011**, P. 129; b) L. R. B. Kesselman, S. Shinwary, P. R. Selvaganapathy, T. Hoare, *Small* **2012**, 8, 1092; c) M. Das, H. Zhang, E. Kumacheva, *Annu. Rev. Mater. Res.* **2006**, 36, 117; d) D. Parasuraman, M. J. Serpe, *ACS Appl. Mater. Interfaces* **2011**, 3, 2732; e) A. Wang , Y. Cui , J. Li , J. C. M. van Hest, *Adv. Funct. Mater.* **2012**, 22, 2673; f) K. Iwai, Y. Matsumura, S. Uchiyamaab, A. P. de Silva, *J. Mater. Chem.* **2005**, 15, 2796; g) G. Huang, Z. Hu, *Macromolecules* **2007**, 40, 3749; h) D. Wang, T. Liu, J. Yin, S. Liu, *Macromolecules* **2011**, 44, 2282.

3 a) R. Contreras-Caceres, S. Abalde-Cela, P. Guardia-Giros, A. Fernandez-Barbero, J. Perez-Juste, R. A. Alvarez-Puebla, L. M. Liz-Marzan, *Langmuir* **2011**, 27, 4520; b) Y. Lu, J. Yuan, F. Polzer, M. Drechsler, J. Preussner, *ACSnano* **2010**, 4, 7078; c) F. Tang, N. Ma, L. Tong, F. He, L. Li, *Langmuir* **2012**, 28, 883.

4 a) T. Welton, *Chem. Rev.* **1999**, 99, 2071; b) T. Torimoto, T. Tsuda, K. Okazaki, S. Kuwabata, *Adv. Mater.* **2010**, 22, 1196.

5 R. D. Rogers, K. R. Seddon, *Science* **2003**, 302, 792.

6 a) C. H. Lee, H. S. Lim, J. Kim, J. H. Cho, *ACSnano*, **2011**, 5, 7397; b) M. T. Rahman, Z. Barikbin, A. Z. M. Badruddoza, P. S. Doyle, S. A. Khan, *Langmuir*, **2013**, 29, 9535; c) M. Tokuda, T. Shindo, H. Minami, *Langumir*, **2013**,29,11284; d) H. Gu, J. Texter, *Polymer*, **2014**, 55, 3378.

7 a) S. G. Lee, *Chem. Commun.* **2006**, 1049; b) Z. Fei, T. J. Geldbach, D. Zhao, P. J. Dyson, *Chem.-Eur. J.* **2006**, 12, 2122.

8 a) Q. Chen, S. C. Bae, S. Granick, *Nature*, **2011**, 469 , 381-384; b) Q. Chen, J. K. Whitmer, S. Jiang, S. C. Bae, E. Luijten, S. Granick, *Science*, **2011**, 331, 199-202.

9 a) J. Texter, *Macromol. Rapid. Commun.* **2012**, 33, 1996; b) J. Y. Yuan, D. Mecerreyes, M. Antonietti, *Prog. Polym. Sci.* **2013**, 38, 1009.

10 a) S. Q. Xu, Z. H. Nie, M. Seo, P. Lewis, E. Kumacheva, H. A. Stone, P. Garstecki, D. B. Weibel, I. Gitlin and G. M. Whitesides, *Angew. Chem., Int. Ed.* **2005**, 44, 724; b) E. Tumarkin, E. Kumacheva, *Chem. Soc. Rev.* **2009**, 38, 2161; c) S. Seiffert, *Macromol. Rapid. Commun.* **2011**, 32, 1600; e) Y. J. Zhao, X. W. Zhao, C. Sun, J. Li, R. Zhu, Z. Z. Gu, *Anal. Chem.* **2008**, 80, 1598.

11 C. Serra, N. Berton, M. Bouquey, L. Prat, G. Hadziioannou, *Langmuir* **2007**, 23, 7745.

12 a) R. Marcilla, M. S. Paniagua, B. L. Ruiz, E. L. Cabarcos, E. Ochoteco, H. Grande, D. Mecerreyes, *J. Polym. Sci. Part A*, **2006**, 44, 3958; b) R. Marcilla, J. A. Blazquez, R. Fernandez, H. Grande, J. A. Pomposo, D. Mecerreyes, *Macromol. Chem. Phys.* **2005**, 206, 299.

13 a) E. Bianchi, R. Blaak, C. N. Likos, Phys. *Chem. Chem. Phys.* **2011**, 13, 6397; b) A. B. Pawar, I. Kretzschmar, *Macromol. Rapid. Commun*. **2010**, 31, 150.

14 a) T. Kaufmann, M. T. Gokmen, C. Wendeln, M. Schneiders, S. Rinnen, H. F. Arlinghaus, S. A. F. Bon, F. E. Du Prez, B. J. Ravoo, *Adv. Mater*. **2011**, 23, 79; b) J. Cui, W. Zhu, N. Gao, J. Li, H. Yang, Y. Jiang, P. Seidel, B. J. Ravoo and G. Li, *Angew. Chem., Int. Ed.,* **2014**, 53, 3844.

15 H. S. Schrekker, M. A. Gelesky, M. P. Stracke, C. M. L. Schrekker, G. Machado, S. R. Teixeira, J. C. Rubim, J. Dupont, *J. Colloid Interface Sci.* **2007**, 316, 189.

16 D. L. Long, R. Tsunashima, L. Cronin, *Angew. Chem. Int. Ed.* **2010**, 49, 1736.

17 K. Yamaguchi, C. Yoshida, S. Uchida, N. Mizuno, *J. Am. Chem. Soc.* **2005**,127, 530.

18 C. Rocchiccioli-Deltcheff, M. Fournier, R. Frank, R. Thouvenot, *Inorg. Chem.* **1983**, 22, 207.

19 a) A. Grossmann, D. Enders, *Angew. Chem. Int. Ed.* **2012**, 51, 314; b) V. Nair, S. Bindu, V. Sreekumar, *Angew. Chem. Int. Ed*. **2004**, 43, 5130; c) A.J . Arduengo III, R.L. Harlow, M.K. Kline, *J. Am. Chem. Soc*. **1991**, 113, 361; d) A. J. Arduengo III, J. R. Goerlich, W. J. Marshall, J. Am. Chem. Soc. **1995**, 117, 11027 ; e) A. J.Arduengo III, R.Krafczyk , R.Schmutzler , *Tetrahedron*, **1999**, 55, 14523.

20 H. Zhou, W. Z. Zhang, Y. M. Wang, J. P. Qu, X. B. Lu, *Macromolecules* **2009**, 42, 5419.

21 J. Jang, J. Bae, *Angew. Chem. Int. Ed.* **2004**, 43, 3803.

22 W.X. Zhang, J. C. Cui, C. A. Tao, C. X. Lin, Y. G. Wu, G. T. Li, *Langmuir* **2009**, 25, 8235.

23 C. Zhao, H. Z. Wang, N. Yan, C. X. Xiao, X. D. Mu, P. J. Dyson, Y. Kou, *J. Catal*. **2007**, 250, 33.